

## Supporting Information

### **Bistable isoelectric point photoswitching in green fluorescent proteins observed by dynamic immunoprobed isoelectric focusing**

Alex J. Hughes\*<sup>†</sup>, Augusto M. Tentori\*<sup>†</sup>, Amy E. Herr\*

\*Department of Bioengineering and the UC Berkeley – UCSF Graduate Program in Bioengineering, University of California, Berkeley, CA 94720.

<sup>†</sup>These authors contributed equally to this work.

## Focusing Model

A 1D isoelectric focusing model assuming linear  $pH$  gradient, constant applied electric field and mobility slope, and equal diffusivities and mobility slopes for  $\beta$  and  $\beta'$  was adapted from that of Weiss et al.<sup>1</sup> with the provision for first-order interconversion between the two populations. Modeling was performed via MATLAB using the “pdepe” solver. Dirichlet boundary conditions specified zero population concentrations at channel edges. Initial conditions were arbitrary Gaussians. Least-squares fitting to experimental data required arbitrary fluorescence normalization of model output for each UV intensity, since the model does not consider  $pH$  and concentration effects on the bright state fluorescence (see Figure S4). Global fitting was conducted over a  $100 \times 100$  mesh in the  $(k_{\beta \rightarrow \beta'}, k_{\beta' \rightarrow \beta})$  parameter space, with the optimal fit returned as that with the lowest sum of pixel-wise squared fluorescence intensity differences between model and experiment bright state distributions. The governing equations were:

$$\frac{dC_{\beta}}{dt} = p_{\beta}(x - x_{pI,\beta})E_x \frac{dC_{\beta}}{dx} + D_{\beta} \frac{d^2C_{\beta}}{dx^2} - k_{\beta \rightarrow \beta'}C_{\beta} + k_{\beta' \rightarrow \beta}C_{\beta'} \quad (1)$$

$$\frac{dC_{\beta'}}{dt} = p_{\beta'}(x - x_{pI,\beta'})E_x \frac{dC_{\beta'}}{dx} + D_{\beta'} \frac{d^2C_{\beta'}}{dx^2} - k_{\beta' \rightarrow \beta}C_{\beta'} + k_{\beta \rightarrow \beta'}C_{\beta} \quad (2)$$

Non-dimensionalizing via the following substitutions:

$$C_0 = C_{\beta} + C_{\beta'} \quad (3)$$

$$\tilde{C}_{\beta} = \frac{C_{\beta}}{C_0} \quad (4)$$

$$\tilde{C}_{\beta'} = \frac{C_{\beta'}}{C_0} \quad (5)$$

$$\Delta x_{pI} = x_{pI,\beta'} - x_{pI,\beta} \quad (6)$$

$$\tilde{x} = \frac{x}{\Delta x_{pI}} \quad (7)$$

$$\tilde{t} = \frac{t}{(\Delta x_{pI})^2/D} \quad (8)$$

Gives:

$$\frac{d\tilde{C}_{\beta}}{d\tilde{t}} = \frac{p\Delta x_{pI}^2 E_x}{D} \left( \tilde{x} - \frac{x_{pI,\beta}}{\Delta x_{pI}} \right) \frac{d\tilde{C}_{\beta}}{d\tilde{x}} + \frac{d^2\tilde{C}_{\beta}}{d\tilde{x}^2} - \frac{k_{\beta \rightarrow \beta'} \Delta x_{pI}^2}{D} \left( \tilde{C}_{\beta} - \frac{k_{\beta' \rightarrow \beta}}{k_{\beta \rightarrow \beta'}} \tilde{C}_{\beta'} \right) \quad (9)$$

$$\frac{d\tilde{C}_{\beta'}}{d\tilde{t}} = \frac{p\Delta x_{pI}^2 E_x}{D} \left( \tilde{x} - \frac{x_{pI,\beta'}}{\Delta x_{pI}} \right) \frac{d\tilde{C}_{\beta'}}{d\tilde{x}} + \frac{d^2\tilde{C}_{\beta'}}{d\tilde{x}^2} + \frac{k_{\beta \rightarrow \beta'} \Delta x_{pI}^2}{D} \left( \tilde{C}_{\beta} - \frac{k_{\beta' \rightarrow \beta}}{k_{\beta \rightarrow \beta'}} \tilde{C}_{\beta'} \right) \quad (10)$$

Thus, the following parameters emerge:

$$Pe = \frac{p\Delta x_{pI}^2 E_x}{D} \quad (11)$$

$$\kappa = \frac{k_{\beta \rightarrow \beta'} \Delta x_{pI}^2}{D} \quad (12)$$

$$\gamma = \frac{k_{\beta' \rightarrow \beta}}{k_{\beta \rightarrow \beta'}} \quad (13)$$

Substituting (11)-(13) into (9) and (10):

$$\frac{d\tilde{C}_\beta}{d\tilde{t}} = Pe \left( \tilde{x} - \frac{x_{pI,\beta}}{\Delta x_{pI}} \right) \frac{d\tilde{C}_\beta}{d\tilde{x}} + \frac{d^2\tilde{C}_\beta}{d\tilde{x}^2} - \kappa(\tilde{C}_\beta - \gamma\tilde{C}_{\beta'}) \quad (14)$$

$$\frac{d\tilde{C}_{\beta'}}{d\tilde{t}} = Pe \left( \tilde{x} - \frac{x_{pI,\beta'}}{\Delta x_{pI}} \right) \frac{d\tilde{C}_{\beta'}}{d\tilde{x}} + \frac{d^2\tilde{C}_{\beta'}}{d\tilde{x}^2} + \kappa(\tilde{C}_\beta - \gamma\tilde{C}_{\beta'}) \quad (15)$$

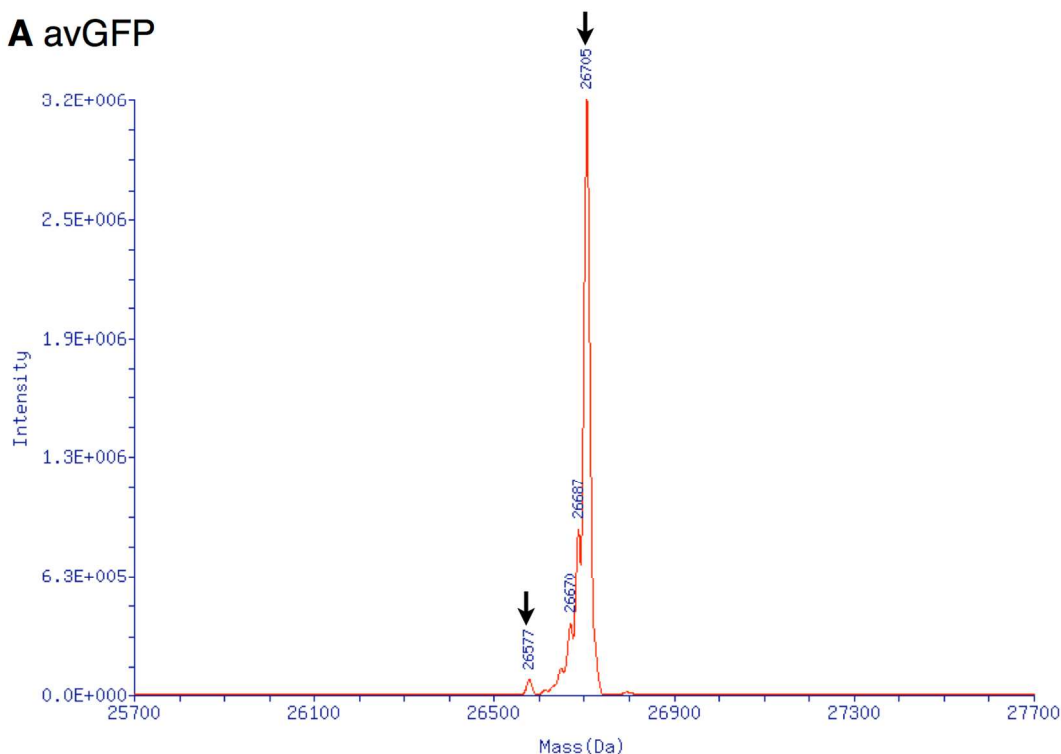
Dimensions are re-introduced as necessary via the following experimentally measured parameters:

$$\begin{aligned} \frac{dx}{d(pH)} &= 10^{-3} \text{ m (pH unit)}^{-1} \\ E_x &= 400 \text{ V cm}^{-1} \\ pI_\beta &= 5.00 \\ pI_{\beta'} &= 5.45 \\ D &= 2.05 \times 10^{-11} \text{ m}^2 \text{ s}^{-1} \\ p &= 2.61 \times 10^{-6} \text{ ms}^{-1} \text{ V}^{-1} \end{aligned}$$

The diffusivity value  $D$  was determined by Gaussian fitting of GFP during defocusing from the IEF-focused state<sup>2</sup>. The mobility slope  $p$  was determined from the measured standard deviation  $\sigma$  of the focused GFP  $\beta$  peak since  $p = D/\sigma^2 E_x$  during steady-state focusing<sup>3</sup>.

## Supplementary Figures

### A avGFP



### B acGFP

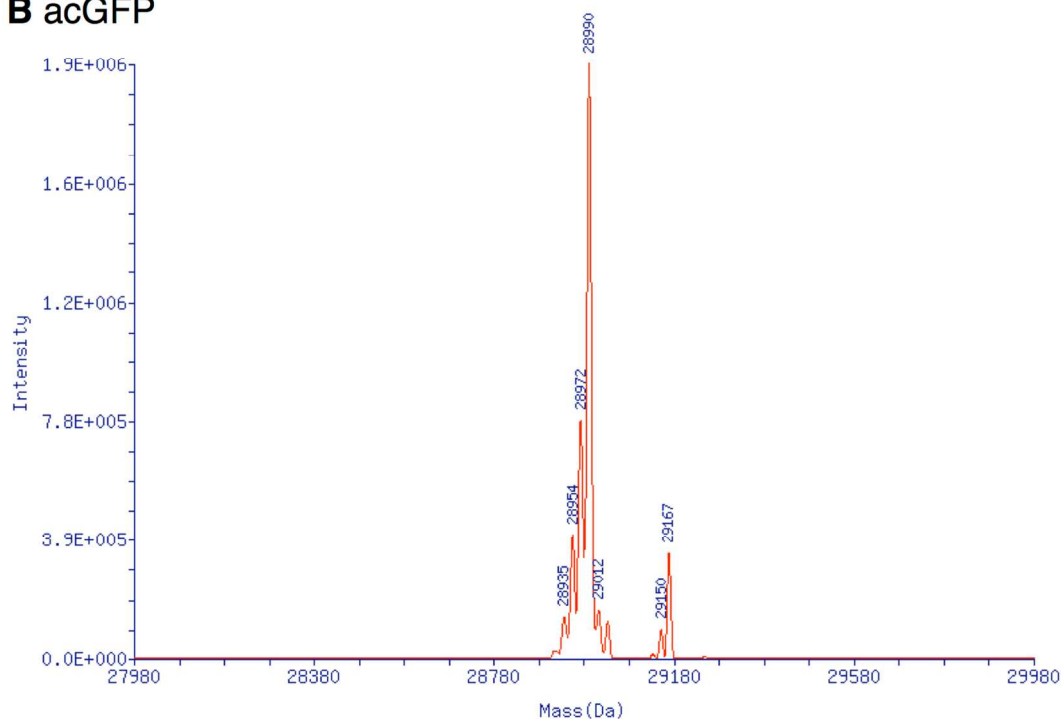


**Figure S1.** Deconvoluted intact mass spectra for purified, recombinant avGFP and acGFP (632373 and 632502, Clontech, Mountain View, CA). The avGFP spectrum shows a major peak at 26,705 Da (black arrow), with dehydration adducts at 26,687 and 26,670 Da. The peak at 26,577 Da (black arrow) is distinct from the major peak by 128 Da, the mass of the C-terminal lysine reported to be cleaved by non-specific protease activity during bacterial expression<sup>4</sup>. Distinct isoform-specific mass differences were not resolved in the case of acGFP. N.B. the mass scales in each graph are not the same.

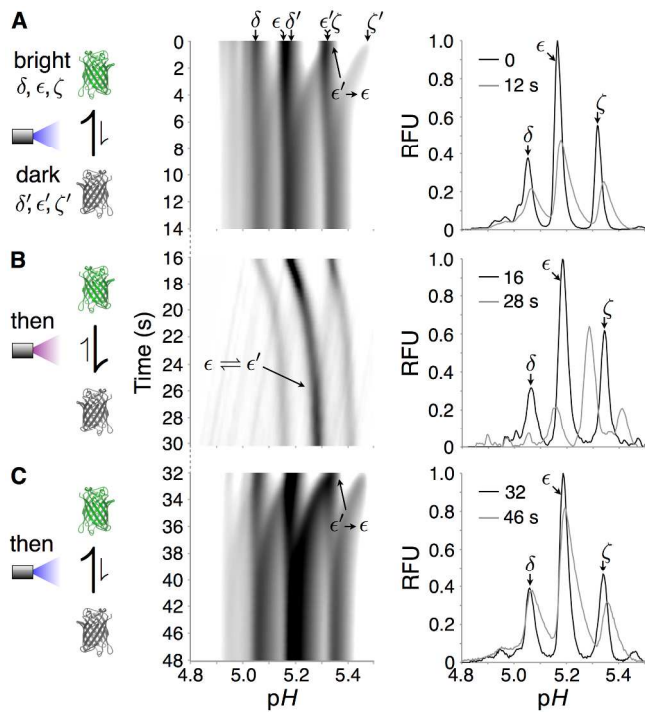


**Figure S2.** Real-time observation of isoelectric point photoswitching in acGFP. Experimental details are identical to those in Figure 3.

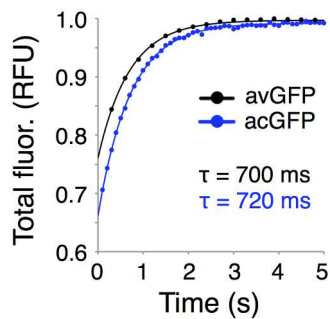


**Figure S3.** Kinetics of reversible photobleaching. Fast total fluorescence recovery under focusing conditions and blue light illumination measured after 10 s pre-exposure of avGFP and acGFP bands to 100% UV light via 10x objective. Single exponential fits of the form  $\text{RFU} = a(1 - e^{-t/\tau}) + b$  are shown for each recovery trace.

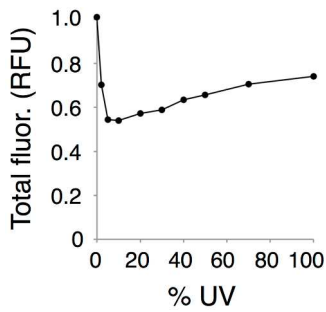


**Figure S4.** avGFP isoform fluorescence during steady-state focusing under UV illumination. Equilibrium between bright and dark populations at  $\mathbf{V}_{avGFP} \sim 2.9$  is reached at  $\sim 5\%$  UV intensity (see Figure 5), producing an initial drop in the total observed fluorescence as the dark population is generated. The total fluorescence then rises rather than remaining constant, perhaps due to concentration and  $pH$  dependencies of GFP brightness in the vicinity of its  $pI^4$ . The concentration dependence (15% increase in extinction coefficient at 395 nm from 7-370  $\mu\text{M}^4$ ) would also explain the greater-than-expected drop in fluorescence during the initial approach to equilibrium, as the isoforms adopt their widest distributions (and thus lowest mean concentrations) in the low UV range. N.B. the local GFP concentration during focusing in these experiments is expected to be in the 10-100  $\mu\text{M}$  range.

## References

- (1) Weiss, G. H.; Catsimpoolas, N.; Rodbard, D. *Arch Biochem Biophys* **1974**, *163*, 106.
- (2) Hughes, A. J.; Lin, R. K. C.; Peehl, D. M.; Herr, A. E. *Proc Natl Acad Sci USA* **2012**, *109*, 5972.
- (3) Rilbe, H. *Ann NY Acad Sci* **1973**, *209*, 11.
- (4) Ward, W. W. In *Green Fluorescent Protein: Properties, Applications and Protocols*; Chalfie, M., Kain, S. R., Eds.; John Wiley & Sons: Hoboken, NJ, 2006.